

SHOCK ACCELERATION OF SOLAR ENERGETIC PROTONS: THE FIRST 10 MINUTES

C. K. NG¹ AND D. V. REAMES

NASA Goddard Space Flight Center, Code 661, Greenbelt, MD 20771; Chee.Ng@nasa.gov, Donald.V.Reames@nasa.gov

Received 2008 August 5; accepted 2008 September 3; published 2008 September 11

ABSTRACT

Proton acceleration at a parallel coronal shock is modeled with self-consistent Alfvén wave excitation and shock transmission. 18–50 keV seed protons at 0.1% of plasma proton density are accelerated in 10 minutes to a power-law intensity spectrum rolling over at 300 MeV by a 2500 km s⁻¹ shock traveling outward from 3.5 r_{\odot} , for typical coronal conditions and low ambient wave intensities. Interaction of high-energy protons of large pitch angles with Alfvén waves amplified by low-energy protons of small pitch angles is key to rapid acceleration. Shock acceleration is not significantly retarded by sunward streaming protons interacting with downstream waves. There is no significant second-order Fermi acceleration.

Subject headings: acceleration of particles — shock waves — Sun: coronal mass ejections (CMEs) — Sun: particle emission

1. INTRODUCTION

Solar energetic particle (SEP) acceleration by coronal mass ejection (CME) driven shocks is an outstanding problem in space weather and astrophysics. Observations indicate that SEPs are accelerated to GeVs in ≤ 10 minutes after CME launch in many events. This short timescale requires mean free paths $\lambda \leq 1 \times 10^{-6}$ AU in diffusive shock acceleration models, whereas $\lambda \geq 0.2$ AU is deduced from interplanetary (IP) transport of SEPs (Bieber et al. 1994). Waves excited by streaming SEPs resolve this paradox. Self-amplified Alfvén waves were invoked in the confinement (Wentzel 1974) and shock acceleration of cosmic rays (Bell 1978). Steady-state models with self-consistent Alfvén waves were applied successfully at the Earth’s bow shock and traveling IP shocks (Lee 1982, 1983, 2005; Gordon et al. 1999). Ng & Reames (1994) showed theoretically that self-amplified waves limit SEP intensity at 1 AU in large events. Reames & Ng (1998) inferred streaming-limited SEP intensities and their radial dependence from *Helios* and *GOES* data. Ng et al. (1999) and Reames et al. (2000) showed how proton-amplified waves control abundance evolution in SEP events. Can streaming SEPs amplify Alfvén waves upstream of CME-driven coronal shocks by $\geq 10^5$ in a few minutes and to what energy are the SEPs accelerated? The answer requires a time-dependent model that treats self-consistently the nonlinear, coupled evolution of SEPs and Alfvén waves. SEP acceleration at a CME-driven shock is a very complex phenomenon (Lee 2005; Cliver et al. 2004; Reames 1999). Researchers have studied different aspects theoretically with various simplifying assumptions, using various analytical and numerical techniques. Significant progress has been made with many issues under lively debate. The reader is referred to Tylka & Lee (2006), Zank et al. (2006), and Giacalone (2005) for the effects of shock geometry; Zank et al. (2007) for the excellent work performed by their group; and Giacalone & Neugebauer (2008) for the effects of a rippled shock.

In this Letter we address the question of how rapid and to what energy a fast parallel shock accelerates SEPs in typical coronal conditions by solving numerically the coupled evolution of SEPs and Alfvén waves. We also address the issues of whether shock acceleration is significantly retarded by SEP damping of outward waves and excitation of inward waves

downstream of the shock (Vainio 2001; Ng 2007) and whether second-order Fermi acceleration plays a significant role. Our model includes in SEP transport: focusing, convection, adiabatic deceleration, pitch-angle scattering, and momentum diffusion due to scattering by counterstreaming Alfvén waves. Treatment of Alfvén waves includes propagation, SEP-driven growth and damping, and shock transmission (Vainio & Schlickeiser 1999). A unique feature of the numerical model is the implementation of the pitch-angle dependent cyclotron resonance condition to calculate self-consistent SEP scattering and Alfvén wave growth. This feature is key to initiating SEP acceleration above the “knee” energy E_{knee} . Momentum diffusion governed by the diffusion tensor elements $D_{\mu\mu}$, $D_{\mu P} = D_{P\mu}$, D_{PP} (Ng et al. 2003) is solved by using an iterative method more accurate than the direct method employed in Ng (2007). Larger rigidity (P) and wavenumber (k) ranges are used to reach higher energy.

Our model accounts for wave evolution time and does not adopt an instantaneous steady-state upstream (US) wave spectrum (Li et al. 2005). The model of Vainio & Laitinen (2007) treats US wave growth and accelerates protons to tens of MeV in 10 minutes. They exclude the downstream (DS) region by reflecting SEPs from the shock statistically. The DS region is an important part of our consideration. We report results for a strong 2500 km s⁻¹ shock starting at 3.5 r_{\odot} , as shock acceleration is reportedly most efficient above $\sim 3 r_{\odot}$ (Cliver et al. 2004). Studies on the dependence on shock, plasma, and turbulence parameters will be published in a full paper. We describe the model in § 2, present the results in § 3, and close with a discussion in § 4.

2. THE MODEL

The model of Ng et al. (2003) is generalized to treat SEP shock acceleration and shock transmission of Alfvén waves in a computational box comoving with the shock. Radial geometry is assumed with mean magnetic field $B = B_0(r_0/r)^2$, plasma proton density $n_H = n_{H,0}(r_0/r)^2$, hence Alfvén velocity $V_A = V_{A,0}(r_0/r)$, where B_0 , $n_{H,0}$, and $V_{A,0}$ are values at $r_0 = 3.5 r_{\odot}$. The evolution of the SEP distribution is governed by

$$\begin{aligned} & \partial_t F + \partial_x(\dot{x}F) + \partial_\mu(\dot{\mu}F) + \partial_e(\dot{e}F) \\ & = \begin{bmatrix} \partial_\mu \\ \partial_e \end{bmatrix}^T \begin{bmatrix} D_{\mu\mu} & D_{\mu e} \\ D_{e\mu} & D_{ee} \end{bmatrix} \begin{bmatrix} \partial_\mu(\chi F) \\ P^3 \partial_e(\chi F P^{-3}) \end{bmatrix}, \end{aligned} \quad (1)$$

¹ Astronomy, University of Maryland, College Park, MD 20742.

$$\dot{x} = \chi(\mu v + W_+) - V_{\text{sh}}, \quad (2)$$

$$\dot{\mu} = (1 - \mu^2)[r^{-1}\chi(v + \mu W_+) - v^{-1}dW_+/dt], \quad (3)$$

$$\dot{\varrho} = \dot{P}/P = -r^{-1}\chi W_+(1 - \mu^2) - \mu v^{-1}dW_+/dt, \quad (4)$$

where $F(P, \mu, x, t) = (B_0/B)(P/P_0)^3 f(P, \mu, x, t)$; f = proton phase-space density in mixed coordinates: distance x from shock and time t in the Sun's inertial frame; P , proton velocity v , and pitch-angle cosine μ in the local outward wave frame moving with velocity $W_+(x, t) = V_{\text{sw}} + V_A$ relative to the Sun. Here $dW_+/dt \equiv \partial_t W_+ + \dot{x} \partial_x W_+$; $\chi = (1 + \mu v W_+/c^2)^{-1}$; $\varrho = \ln(P/P_0)$; $P_0 = \text{constant}$; $D_{\mu\varrho} = D_{\varrho\mu} = P^{-1}D_{\mu P}$, $D_{\varrho\varrho} = P^{-2}D_{PP}$; $r(x, t) = x + r_{\text{sh}}(t)$; $r_{\text{sh}}(t)$ = shock radius; $V_{\text{sh}} = \text{constant}$ shock velocity. The plasma velocity $V_{\text{sw}}(x) = V_d$ at $x < 0$ (DS) and $V_{\text{sw}}(x) = V_u$ at $x > 0$ (US). Besides focusing and adiabatic deceleration, equations (3) and (4) include the differential frame transformation of (μ, P) following particle motion. The shock jump in $W_+(r, t)$ gives a P -increment for almost all shock-crossing particles (eq. [4]).

We consider only right- and left-hand circularly polarized, inward and outward parallel propagating Alfvén waves. The ambient outward wave magnetic intensities $I^{R+} = I^{L+} \propto k^{-5}$ are specified for US and DS separately via steady-state solutions to the wave kinetic equation. As outward waves dominate near the Sun, we specify $I^{R-} = I^{L-} = 0.05I^{R+}$. I^σ , n_{H} , and V_A are then modified for the shocked DS region assuming 10 s shock transmission before seed-particle injection at $t = 0$. Wave evolution is governed by the wave kinetic equation

$$\partial_t \Psi_\sigma + \partial_x [(W_\sigma - V_{\text{sh}})\Psi_\sigma] + \eta \partial_\eta (V_\eta^\sigma \Psi_\sigma) = \gamma_\sigma \Psi_\sigma, \quad (5)$$

with wave action density $\Psi_\sigma(\eta, x, t) = 2I^\sigma(\eta, x, t)\eta|W_\sigma|/(\eta_0 V_A)$, $\eta = k/B$, $\eta_0 = \text{constant}$, $V_\eta^\sigma = 2W_\sigma/r - dW_\sigma/dr$, $\gamma_\sigma = \text{fractional growth rate of } I^\sigma$, $W_\sigma = W_+$ for $\sigma = R+, L+$, and $W_\sigma = W_- = V_{\text{sw}}(r, t) - V_A(r, t)$ for $\sigma = R-, L-$. Equations (1) and (5) are coupled via

$$D_{\mu\mu} = \sum_\sigma D_{\mu\mu}^\sigma = \sum_\sigma \frac{v^2}{4P^2} \int dk R_{\mu\mu}^\sigma I^\sigma, \quad (6)$$

$$\gamma_\sigma(k, r, t) = 2\pi^2 c e^3 g_\sigma V_A \int \int d\mu dP R_{\mu\mu}^\sigma Gf, \quad (7)$$

where $Gf \equiv P^3[\mathcal{E}(1 - \mu V_\sigma/v)]^{-2}[\partial_\mu f - (V_\sigma/v)(\mu \partial_\mu f - \partial_\eta f)]$; $\mathcal{E} = \text{total particle energy}$; $g_\sigma = 1$, $V_\sigma = 0$ for $\sigma = R+, L+$; and $g_\sigma = -1$, $V_\sigma = -2V_A$ for $\sigma = R-, L-$. The wave-particle resonance function $R_{\mu\mu}^\sigma(\mu, P, k, V_A, B)$ (Ng & Reames 1995; Ng et al. 2003) includes minimal broadening of the quasi-linear resonance condition $k = B/[P(\mu - V_\sigma/v)]$.

At the initial shock location at $r = 3.5 r_\odot$, we specify $V_u = 83 \text{ km s}^{-1}$, $n_{\text{H},0} = 2 \times 10^5 \text{ cm}^{-3}$, $V_{A,0} = 700 \text{ km s}^{-1}$ from the semiempirical models of Guhathakurta et al. (1999). Hence $B_0 = 0.143 \text{ G}$, consistent with results from gyrosynchrotron emission (Dulk & McLean 1978). Prescribed ambient $I^\sigma \propto k^{-1.5}$ gives $\lambda = 0.23 \text{ AU}$ at 1 MeV (0.68 AU at 100 MeV).

Constant $V_d = 1880 \text{ km s}^{-1}$, $V_{\text{sh}} = 2500 \text{ km s}^{-1}$, and V_u in the Sun's inertial frame are assumed, giving a fluid compression ratio $c_f = 3.895$ and an initial Alfvén Mach number $M_A = 3.45$ increasing to 5.56 at $t = 10$ minutes, when $r_{\text{sh}} = 5.65 r_\odot$. The relation between c_f , M_A , plasma beta = 0.1, and relative wave amplitude (Vainio & Schlickeiser 1999) is satisfied at $t = 0$ but not at $t > 0$. The back reaction of SEPs and amplified waves on shock evolution is not considered.

For quasi-parallel shocks, Zank et al. (2001) obtain 2% reflection of solar-wind protons by cross-shock electric potential to $\geq 3E_{\text{ramp}}$. Here $3E_{\text{ramp}} = 90 \text{ keV}$. From the observed postshock proton distribution in the 1978 August 27 event (Gosling et al. 1981, Figs. 4 and 6), we find tail density above 18 keV is $b = 0.0002$ times the observed $n_{\text{H}} = 25 \text{ cm}^{-3}$. Larger b is expected in the strongly heated plasma DS of the 2500 km s^{-1} shock. There may also be suprathermal remnants from previous SEP events (Mason et al. 1999; Tylka et al. 2001). Guided by the above, we prescribe DS isotropic seed protons

$$f_{\text{inj}} = bn_{\text{H}}(x_0)(\alpha - 3)P^{-\alpha}/[4\pi(P_a^{3-\alpha} - P_b^{3-\alpha})], \quad (8)$$

at $P_a < P < P_b$, with injection fraction $b = 0.001$, $\alpha = 5$, $P_a = 6 \text{ MV}$ (18 keV), and $P_b = 9.8 \text{ MV}$ (50 keV). Since $P_b < P_1 = 10.4 \text{ MV}$, the lowest grid rigidity, the DS seeds emerge US as proton beams from 10.4 to 14.7 MV (57 to 115 keV).

Each shock-crossing US wave $I_u(k_u)$ is converted to two DS waves $I_d(k_d)$ of the same helicity:

$$I_d(k_d)/I_u(k_u) = (1 + \zeta_u \zeta_d / \sqrt{c_j})^2 c_w / 4, \quad (9)$$

with wave compression ratio $c_w \equiv k_d/k_u = c_f(M_A - \zeta_u)/(M_A - \zeta_d \sqrt{c_j})$, $\zeta_u = \pm 1$ and $\zeta_d = \pm 1$ for outward (inward) US and DS waves (Vainio & Schlickeiser 1999; Webb et al. 1999). Since wave growth is limited by nonlinear processes, we impose $I^\sigma(k) \leq I_{\text{sat}}(k) = B^2/(3\pi k)$ so that $\lambda \geq 3r_g$ while preserving the ratio of transmitted inward and outward waves. Shock transmission produces only a small fraction (5%) of DS inward wave intensity.

The numerical grid is $x_j = 2.15 \times 10^{-4}(j - 1/2) r_\odot$, $j = -200$ to 800; $\mu_i = 0.05(i + 1/2)$, $i = -20$ to 19; $\varrho_\ell = \varrho_1 + 0.08664(\ell - 1)$, $\ell = 1$ to 60, $P_1 = 10.38 \text{ MV}$; and $\log \eta_m = \log \eta_1 + 0.05(m - 1)$, $m = 1$ to 58, $\eta_1 = 5.465 \times 10^{-4} \text{ MV}^{-1}$. At the boundaries, exterior $F = \text{interior } F$. At the outer boundary, exterior $I^\sigma = \text{interior } I^\sigma$. The μ and P increments of shock-crossing protons are evaluated by frame transformation. Equations (1) and (5) are solved with dynamic time steps using operator splitting and locally one-dimensional differencing (Ng et al. 2003); (μ, P) -diffusion is solved iteratively.

3. RESULTS

In 600 s, the 2500 km s^{-1} parallel shock accelerates 18–50 keV DS seed protons to a power-law intensity spectrum j_E extending to $E_{\text{knee}} \sim 300 \text{ MeV}$ (Fig. 1a). The energy spectral index of 0.8 is consistent with $c_w = 6.46$ decreasing to 4.95 between US and DS outward Alfvén waves. At 12.3 MeV, the j_E spatial profile rises swiftly from a spike at 180 s to the steady-state form (Lee 1983): a DS plateau and an US exponential tail at $t > 250 \text{ s}$ (Fig. 1b). This implies negligible second-order Fermi acceleration, consistent with no enhanced inward and outward waves in proximity.

Streaming SEPs US rapidly amplify outward waves and

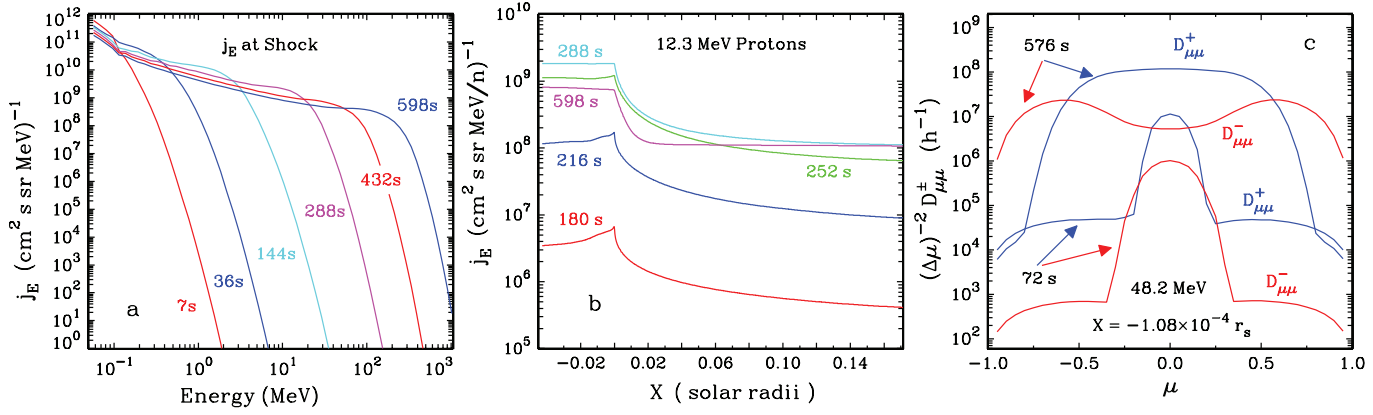


FIG. 1.—(a) Proton intensity spectra at the first US cell. (b) 12.3 MeV proton intensity spatial profiles. (c) 48.2 MeV proton μ -diffusion coefficients $D_{\mu\mu}^{\pm}$ vs. μ due to outward and inward Alfvén waves at the first DS cell at $t = 72$ and 576 s. $\Delta\mu = 1/20$.

damp inward waves. Wave growth extends to low wavenumber k (Fig. 2a) as acceleration proceeds to high energy. The amplified waves enhance scattering, providing a positive feedback that rapidly bootstraps acceleration. The DS outward waves derive from shock-transmitted US outward waves and are shifted to higher k (Fig. 2b; cf. Fig. 2a). The much weaker DS inward waves (not shown) are k -shifted by a smaller amount. The k -shifted enhanced DS waves thus resonate with SEPs of lower values of $P(\mu - V_o/v)$. The effect is seen by comparing $D_{\mu\mu}$ US and DS at $t = 576$ s at five rigidities from 140 to 1449 MV (Figs. 2c, 2d). The hump in each $D_{\mu\mu}$ curve originates from

proton-amplified US waves and occupy a smaller μ range DS than US at $P \geq 1117$ MV. At $P \leq 305$ MV, however, the DS waves at k resonant with large μ are amplified by US SEPs of higher P , so the DS humps are also wide.

How acceleration begins can be seen in the evolution of US and DS μ -distributions (Figs. 2e, 2f). SEPs at $E > E_{knee}$ are first accelerated at the $D_{\mu\mu}$ hump at small $|\mu|$, where resonant waves are available. Some accelerated SEPs US scatter to larger μ and excite US waves at smaller k , which are then transmitted DS. The result is that the DS $D_{\mu\mu}$ hump widens and acceleration extends to higher energy. The μ -dependent resonance condition

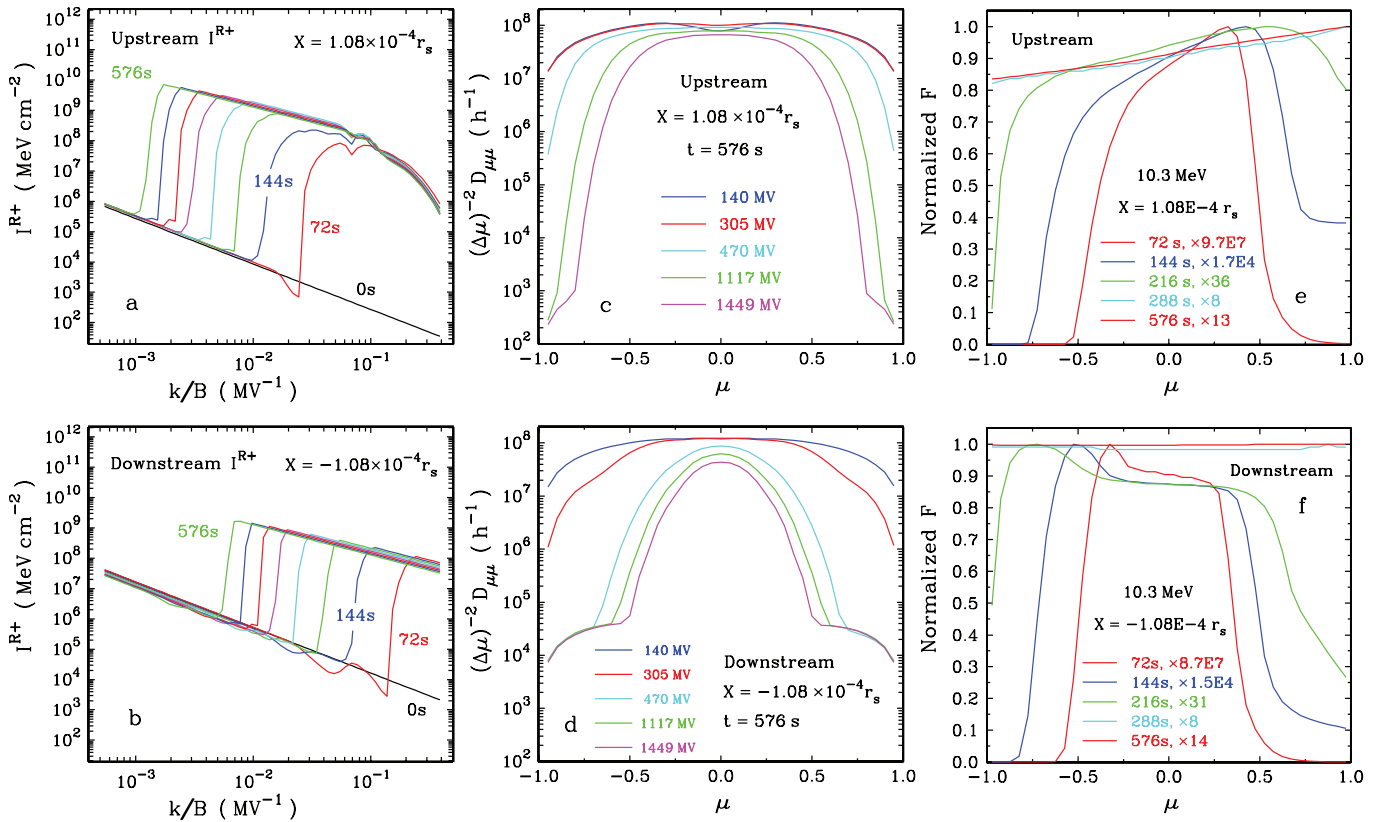


FIG. 2.—Evolution in the first US cell of (a) I^{R+} at 72 s intervals, (c) $D_{\mu\mu}$ at $t = 576$ s at indicated rigidities, and (e) pitch-angle distributions at indicated times. The lower panels (b), (d), and (f) show the same respectively in the first DS cell.

$k \sim B/[P(\mu - V_o/v)]$ is crucial in this process. It allows waves excited by low- P large- μ SEPs to scatter high- P small- μ SEPs (and vice versa).

Do DS inward waves, which scatter SEPs back to the shock with energy loss as seen in outward-wave frame, dominate in the immediate DS and retard acceleration? Figure 1c compares $D_{\mu\mu}^+$ and $D_{\mu\mu}^-$ due to outward and inward waves, respectively, of 48.2 MeV protons in the first DS cell at $t = 72$ and 576 s. At both times, scattering by strong outward waves dominate in the central μ -range, where most of the SEPs are scattered back and forth across the shock. Hence shock acceleration is not significantly retarded by SEP damping (amplification) of DS outward (inward) waves.

4. SUMMARY AND DISCUSSION

Shock acceleration is simulated in a moving box model with the usual processes of SEP transport and momentum diffusion, and the propagation, shock transmission, and SEP-driven evolution of Alfvén waves. For typical coronal conditions and weak ambient waves, a 2500 km s⁻¹ parallel shock starting at 3.5 r_\odot accelerates 18–50 keV DS seed protons at 0.001 n_H to a power-law intensity spectrum with $E_{\text{knee}} \sim 300$ MeV in 10 minutes (Fig. 1a). The box size of 0.215 $r_\odot = 2.8 \times 10^5$ ion inertial lengths and $\Omega t = 8.2 \times 10^5$ for $t = 600$ s are respectively 10 and 140 times larger than in the hybrid simulation of Giacalone (2004).

A key feature of the model is the consistent use of the μ -dependent cyclotron resonance condition $B/k \approx P(\mu - V_A/v)$ to calculate the momentum diffusion tensor $D_{\alpha\beta}$ and the wave growth rate γ_o , so that waves excited by low-energy protons also scatter high-energy ones. Using the μ -dependent condition to calculate γ_o but the “sharpened” condition $B/k = P$ to calculate $D_{\mu\mu}$ underestimates the effect of amplified waves on $D_{\mu\mu}$, giving little acceleration (Berezhko et al. 1998). Using the “sharpened” condition to calculate both γ_o and $D_{\mu\mu}$ (Vainio & Laitinen 2007) requires high-energy protons to amplify unique

resonant waves from the *ambient state* before they experience enhanced scattering. The “sharpened” condition is a compromise on the physics of cyclotron resonant interaction.

The evolution of SEPs and DS inward and outward Alfvén waves shows that (1) second-order Fermi acceleration is not significant, and (2) in the immediate DS, $D_{\mu\mu}^+ \gg D_{\mu\mu}^-$ (Fig. 1c) over the μ -range where *initial* acceleration at $E > E_{\text{knee}}$ occurs, hence SEP interaction with DS waves do not seriously retard acceleration. At $t = 600$ s, SEP energy density $\epsilon_{\text{SEP}} = 7900$ MeV cm⁻³ at $r_{\text{sh}} = 5.65 r_\odot$, falling steeply with x ; shock ramp energy density $\epsilon_{\text{ramp}} = 6100$ MeV cm⁻³, Alfvén-wave magnetic energy density $\epsilon_{\text{wave}} = 470$ MeV cm⁻³, and $B_o^2/8\pi = 510$ MeV cm⁻³. This indicates the shock would be modified, an effect not considered here, and that we are pushing the limits of quasi-linear theory. Reducing injection from $b = 0.001$ to $b = 0.0005$ yields $E_{\text{knee}} \sim 100$ MeV, $\epsilon_{\text{SEP}} = 1950$ MeV cm⁻³, and $\epsilon_{\text{wave}} = 420$ MeV cm⁻³. However, it is impossible to deduce j_E at 1 AU from Figure 1a because of streaming limit (Ng & Reames 1994; Reames & Ng 1998). We plan to inject escaping proton flux from this model into an IP transport model with self-consistent waves (e.g., Ng et al. 2003) to predict j_E at 1 AU.

Detailed study of model dependence on shock, ambient wave, and plasma parameters will be presented in a full paper. Although the model is simplified, neglecting, e.g., shock geometry and wave cascading, it captures the essential role of wave-particle interaction with a realistic description of SEP shock acceleration through self-amplified waves. Faster acceleration to higher energy may be possible at quasi-perpendicular shocks. In future, we will include minor ions and the effects of shock geometry, and integrate the box acceleration model into an IP transport model.

We thank the referee for helpful comments. This work was supported by NASA under LWS-04-0000-0076 and SHP04-0016-0024.

REFERENCES

- Bell, A. R. 1978, MNRAS, 182, 147
 Berezhko, E. G., Petukhov, S. I., & Taneev, S. N. 1998, Astron. Lett., 24, 122
 Bieber, J. W., et al. 1994, ApJ, 420, 294
 Cliver, E. W., Kahler, S. W., & Reames, D. V. 2004, ApJ, 605, 902
 Dulk, G. A., & McLean, D. J. 1978, Sol. Phys., 57, 279
 Giacalone, J. 2004, ApJ, 609, 452
 ———. 2005, ApJ, 628, L37
 Giacalone, J., & Neugebauer, M. 2008, ApJ, 673, 629
 Gordon, B. E., Lee, M. A., Möbius, E., & Trattner, K. J. 1999, J. Geophys. Res., 104, 28263
 Gosling, J. T., et al. 1981, J. Geophys. Res., 86, 547
 Guhathakurta, M., Sittler, E. C., Jr., & McComas, D. 1999, Space Sci. Rev., 87, 199
 Lee, M. A. 1982, J. Geophys. Res., 87, 5063
 ———. 1983, J. Geophys. Res., 88, 6109
 ———. 2005, ApJS, 158, 38
 Li, G., Zank, G. P., & Rice, W. K. M. 2005, J. Geophys. Res., 110, A06104
 Mason, G. M., Mazur, J. E., & Dwyer, J. R. 1999, ApJ, 525, L133
 Ng, C. K. 2007, in AIP Conf. Proc. 932, Turbulence and Nonlinear Processes in Astrophysical Plasmas, ed. D. Shaikh & G. P. Zank (Melville: AIP), 271
 Ng, C. K., & Reames, D. V. 1994, ApJ, 424, 1032
 ———. 1995, ApJ, 453, 890
 Ng, C. K., Reames, D. V., & Tylka, A. J. 1999, Geophys. Res. Lett., 26, 2145
 ———. 2003, ApJ, 591, 461
 Reames, D. V. 1999, Space Sci. Rev., 90, 413
 Reames, D. V., & Ng, C. K. 1998, ApJ, 504, 1002
 Reames, D. V., Ng, C. K., & Tylka, A. J. 2000, ApJ, 531, L83
 Tylka, A. J., & Lee, M. A. 2006, ApJ, 646, 1319
 Tylka, A. J., et al. 2001, ApJ, 558, L59
 Vainio, R. 2001, Proc 27th Int. Cosmic Ray Conf. (Hamburg), 2054
 Vainio, R., & Laitinen, T. 2007, ApJ, 658, 622
 Vainio, R., & Schlickeiser, R. 1999, A&A, 343, 303
 Webb, G. M., Zakharian, A., Briot, M., & Zank, G. P. 1999, J. Plasma Phys., 61, 295
 Wentzel, D. G. 1974, ARA&A, 12, 71
 Zank, G. P., Li, G., & Verkhoglyadova, O. 2007, Space Sci. Rev., 130, 255
 Zank, G. P., et al. 2001, Phys. Plasmas, 8, 4560
 ———. 2006, J. Geophys. Res., 111, A06108